

# Conformation and Selectivity towards Silver of Thiocrown Ethers based on Xylyl Subunits†

Joyce C. Lockhart,<sup>\*a</sup> David P. Mousley,<sup>a</sup> M. N. Stuart Hill,<sup>a</sup> Nicholas P. Tomkinson,<sup>a</sup> Francesc Teixidor,<sup>b</sup> Maria P. Almajano,<sup>b</sup> Luis Escriche,<sup>b</sup> Jaume F. Casabo,<sup>b</sup> Reijo Sillanpää<sup>c</sup> and Raikko Kivekäs<sup>d</sup>

<sup>a</sup> Department of Chemistry, Bedson Building, The University, Newcastle upon Tyne NE1 7RU, UK

<sup>b</sup> UAB, Bellaterra and Institut de Ciència dels Materials de Barcelona, Bellaterra, Spain

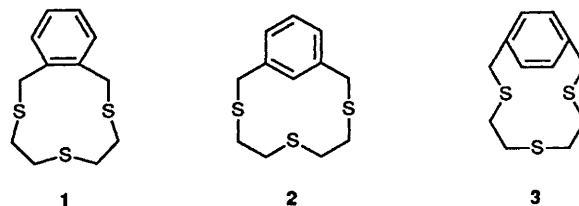
<sup>c</sup> Department of Chemistry, University of Turku, SF-20500, Turku, Finland

<sup>d</sup> Division of Inorganic Chemistry, Department of Chemistry, University of Helsinki, Vuorikatu 20, SF-00100, Helsinki, Finland

Studies intended to relate the conformational behaviour and selectivity (towards silver) of arene thiocrown ether ligands with one fused SCCSCCS unit have been made. The cyclophane isomers 2,5,8-trithia[9]-*o*-benzenophane **1** and 2,5,8-trithia[9]-*p*-benzenophane **3** have been characterised by single-crystal X-ray crystallography: **1**, monoclinic, space group  $P2_1/c$ ,  $a = 8.855(2)$ ,  $b = 15.892(2)$ ,  $c = 9.943(2)$  Å,  $\beta = 111.52(1)^\circ$ ,  $Z = 4$ ,  $R = 0.052$ ,  $R' = 0.046$ , based on 1392 observed reflections; **3**, monoclinic, space group  $P2_1/n$ ,  $a = 10.363(5)$ ,  $b = 7.574(3)$ ,  $c = 16.647(2)$ ,  $\beta = 101.64(2)^\circ$ ,  $Z = 4$ ,  $R = 0.039$ ,  $R' = 0.041$ , based on 1704 observed reflections. New NMR information on solution conformations of **1** and **3** and of the *m*-isomer **2**, is compared with crystal structure data, and with the patterns of conformational change seen when molecular dynamics (MD) simulations are performed on the molecules (using the crystal data as starting conformation). The separations between non-bonded sulfurs in the crystal structures, MD simulations, and in a series of metal complex crystal structures obtained from the Cambridge Structural Database or the literature have been analysed. The MD simulation provides a new perspective on preorganisation of the ligands studied prior to metal-ion co-ordination.

There has been conjecture about the conformation of crown ethers and thioethers, in particular the importance of fluxionality.<sup>1</sup> Studies of this feature have been important to us in relation to the design of ligands for ion-selective electrodes, where it is clear that the kinetics may be important.<sup>2,3</sup> For several simple thiocrown ethers some of us have recently proposed an interpretation of the NMR solution coupling information, and molecular dynamics (MD) simulations. In this paper, similar studies are made of the xylene-based analogues **1–3**, of which some have proved to have special co-ordinating properties for silver ions (**2** and analogues with an oxygen in the bridge) and have been demonstrated to be specially selective for silver in ion-selective electrode (ISE) formulations.<sup>3</sup>

The thiocrown macrocycles have come into great prominence recently, due to their ability to stabilise unusual oxidation states of the transition metals and coinage metals.<sup>4,5</sup> Of particular interest to some of us has been the potential of these ligands as sensors for thiophilic metal ions such as silver,<sup>3</sup> and we consider in this paper the relevance of the conformations in the special selectivity of some of them towards silver as opposed to other thiophilic metal ions. We have noted previously<sup>1</sup> that, from NMR evidence, in solution the structures of thiocrown ethers are not rigid, but flipping rapidly between conformations, and that MD simulations (using a protocol we developed for the purpose) can be used to probe a considerable range of conformations which the molecules are likely to access (as isolated gas-phase molecules). Plots showing the evolution of the torsion angles of the macrocycle on a time-scale of 600 ps were used in the earlier work to show the conformational processes in which the macrocycle might engage.



We have now made a further investigation on thiocrowns, with rigid xylyl units, fused to one SCCSCCS 'bracket' unit,<sup>6</sup> **1–3**. For **2** there was available crystal structure data, although the published coordinates were wrongly printed.<sup>7</sup> The crystal structures of **1** and **3** were obtained in this work, since the published data<sup>7</sup> for **1** did not include the aromatic carbons and were inadequate as input for the molecular simulations. We determined the <sup>1</sup>H NMR spectra, and analysed the coupling patterns to establish the conformational mix of the thioether segments. This reflects the proportion of *gauche* and *anti* SCCS segments in the solution conformation. The behaviour of the molecules was also simulated using molecular mechanics and dynamics. Comparison of the structures determined by X-ray methods and by NMR solution techniques with the simulated structures should allow exploration of the apparent flexibility of these small macrocycles, and the timing of torsional movements relative to that of the ligation process. On the time-scale simulated, it was expected that the movement involving the large xylyl unit would introduce distinctive and higher barriers to torsional movements, other than those observed in the previous simulations.<sup>1</sup>

## Experimental

**Materials.**—The thiocrowns **1–3** were prepared as shown below.<sup>3</sup> Commercially available deuteriated solvents were used (Aldrich).

† Supplementary data available: see Instructions for Authors, *J. Chem. Soc., Dalton Trans.*, 1992, Issue 1, pp. xx–xxv.

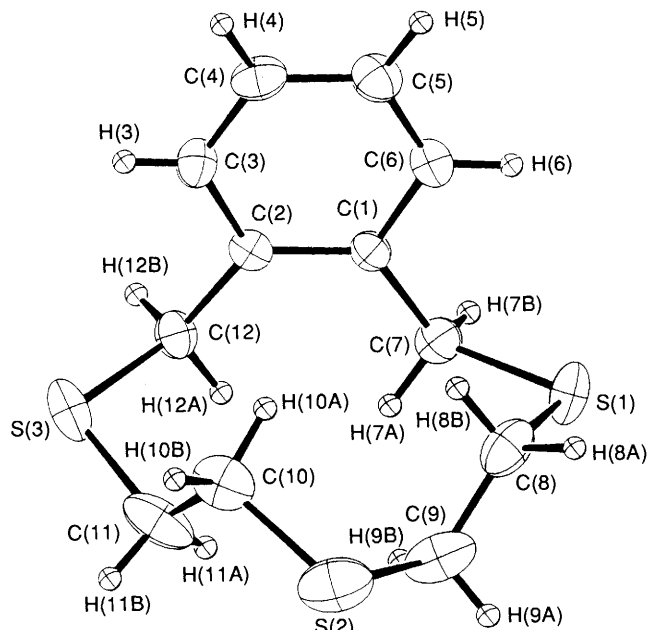


Fig. 1 An ORTEP drawing of compound 1. Thermal ellipsoids are drawn at 30% probability

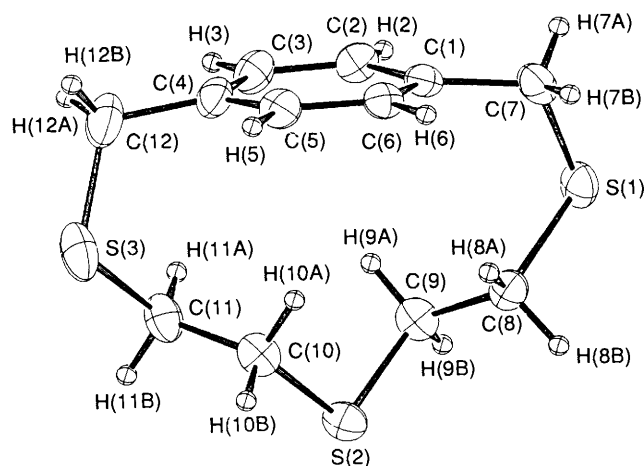


Fig. 2 An ORTEP drawing of compound 3. Thermal ellipsoids are drawn at 30% probability

2,5,8-Trithia[9]-*p*-benzenophane 3. Under a nitrogen atmosphere and high dilution conditions, a solution (A) of potassium hydroxide (0.04 mol) and bis(2-mercaptoethyl) sulfide (0.04 mol) in methanol (50 cm<sup>3</sup>) was mixed over methanol (1.5 dm<sup>3</sup>) with a solution (B) of  $\alpha,\alpha'$ -dichloro-*m*-xylene (0.02 mol) in methanol-tetrahydrofuran (thf) (1:1, 50 cm<sup>3</sup>) at a rate of 3 cm<sup>3</sup> h<sup>-1</sup>. The KCl formed was filtered off and the resulting solution evaporated to dryness. The oily material was extracted with benzene (150 cm<sup>3</sup>), washed with sodium carbonate solution, and dried over sodium sulfate for 8 h. The dry residue was dissolved in benzene (5 cm<sup>3</sup>) and chromatographed over neutral alumina. The fraction eluted with benzene was separated and evaporated to dryness. The resulting yellowish oily material was poured into light petroleum (b.p. 40–60 °C, 50 cm<sup>3</sup>) and a white crystalline compound appeared. Yield 41% (Found: C, 56.3; H, 6.6. C<sub>12</sub>H<sub>16</sub>S<sub>3</sub> requires C, 56.2; H, 6.3%). NMR (CDCl<sub>3</sub>): <sup>1</sup>H,  $\delta$  1.83 (4, m, CCH<sub>2</sub>S), 2.30 (4, m, SCH<sub>2</sub>C), 3.84 (4, s, SCH<sub>2</sub>C<sub>6</sub>H<sub>4</sub>) and 7.38 (4, s, C<sub>6</sub>H<sub>4</sub>); <sup>13</sup>C,  $\delta$  136, 130, 36, 32 and 30.

2,5,8-Trithia[9]-*o*-benzenophane 1. The synthesis was performed as described above for the *para* isomer. This procedure, avoiding the use of dimethylformamide, gave a yield of 45%. The compound had satisfactory characterization as in ref. 7.

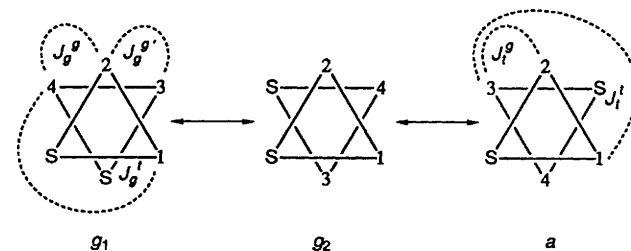
2,5,8-Trithia[9]-*m*-benzenophane was synthesised as in ref. 3.

Table 1 Chemical shift and coupling constant data\* for the SCCS bracket of the thiocyclophanes

| Compound | $\delta_{\text{obs}}$ (A and B) | $J$      | $J'$    | $J_{\text{gem}}$ |
|----------|---------------------------------|----------|---------|------------------|
| 1        | 2.623(A), 2.746(B)              | 8.74(4)  | 5.98(7) | -14.91, -14.85   |
| 2        | 2.222(A), 2.420(B)              | 13.15(8) | 4.51(5) | -14.35(6)        |
| 3        | 1.773(A), 2.247(B)              | 13.07(5) | 4.63(5) | -14.36(6)        |

\* Shifts in ppm,  $J$  in Hz, solvent CDCl<sub>3</sub> unless stated otherwise; standard deviations in parentheses. Simulated with NUMARIT or PANIC.

Table 2 Coupling constants calculated for the SCCS segment in thiocrowns



| Equation*                         | $J(\text{calc.})/\text{Hz}$ |
|-----------------------------------|-----------------------------|
| $J_t^g = 1.35 + 0.63(E_x + E_y)$  | 4.63                        |
| $J_t^t = 18.07 - 0.88(E_x + E_y)$ | 13.49                       |
| $J_g^g = 8.94 - 0.94(E_x + E_y)$  | 4.05                        |
| $J_g^t = 10.45 - 1.43(E_x + E_y)$ | 3.01                        |
| $J_g^t = 16.47 - 0.60(E_x + E_y)$ | 13.35                       |

\* From ref. 10.  $E_x$  and  $E_y$  are the electronegativities of the heteroatoms (in this case sulfur) attached to the CH<sub>2</sub>CH<sub>2</sub> unit.

Table 3 Averaged coupling constants calculated for the SCCS segment in conformer mixtures

| Ratio*      | $J(\text{calc.})/\text{Hz}$ | $J'(\text{calc.})/\text{Hz}$ | Comment                        |
|-------------|-----------------------------|------------------------------|--------------------------------|
| $g_1:g_2:a$ |                             |                              |                                |
| 1:0:0       | 13.35                       | 3.53                         | Fixed <i>gauche</i> rotamer    |
| 1:1:0       | 8.18                        | 3.79                         | All- <i>gauche</i> equilibrium |
| 0:0:1       | 7.024                       | 7.00                         | All- <i>anti</i> equilibrium   |
| 1:1:2       | 8.64                        | 6.40                         | —                              |
| 1:1:3       | 9.61                        | 6.05                         | —                              |
| 1:1:4       | 10.26                       | 5.81                         | —                              |
| 0:0:1       | 13.49                       | 4.63                         | Fixed <i>anti</i> rotamer      |

\* Calculated for possible conformer mixes, assuming classical torsion angles for the SCCS segment.

**NMR Spectroscopy.**—The ligands 1–3 were examined in CDCl<sub>3</sub> solution at 300 (Bruker WB300) and/or 500 MHz (Bruker AMX500). The SCCS segments of each, which gave apparent AA'BB' spectra, were analysed with NUMARIT<sup>8</sup> or PANIC to extract the average coupling constants for the segment.<sup>9</sup> Derived coupling constants appear in Table 1, and calculated values in Tables 2 and 3.

**Crystallography.**—Coordinates for the crystal structure of compound 2 used in the simulations were obtained directly from the Cambridge Crystallographic Data Centre (CCDC):<sup>11</sup> an error in the published atomic coordinates in Table II of p. 4086 of ref. 7 for ligand 2 was corrected by Dave Watson of CCDC.<sup>11</sup> Another structure determination<sup>7</sup> of structure 1 was brought to our attention after the determination to be described below. The coordinates actually used in later molecular mechanics work were those from the present determination, since these gave access to the aromatic carbon coordinates; the determination reported here is based on more reflections.

Crystal data for compounds 1 and 3 with other experimental

**Table 4** Crystallographic data and experimental details for compounds **1** and **3**\*

|                                       | <b>1</b>                                       | <b>3</b>                                       |
|---------------------------------------|--|--|
| Formula                               | C <sub>12</sub> H <sub>16</sub> S <sub>3</sub> | C <sub>12</sub> H <sub>16</sub> S <sub>3</sub> |
| Space group                           | P2 <sub>1</sub> /c                             | P2 <sub>1</sub> /n (alt. P2 <sub>1</sub> /c)   |
| a/Å                                   | 8.855(2)                                       | 10.363(5)                                      |
| b/Å                                   | 15.892(2)                                      | 7.574(3)                                       |
| c/Å                                   | 9.943(2)                                       | 16.647(2)                                      |
| β/°                                   | 111.52(1)                                      | 101.64(2)                                      |
| U/Å <sup>3</sup>                      | 1301.6(7)                                      | 1279.7(7)                                      |
| D <sub>calc</sub> /g cm <sup>-3</sup> | 1.309  | 1.331  |
| μ(Mo-Kα)/cm <sup>-1</sup>             | 5.15   | 5.24   |
| Crystal colour                        | Colourless, prism                              | Colourless, plate                              |
| Crystal dimensions/mm                 | 0.12 × 0.20 × 0.22                             | 0.10 × 0.28 × 0.30                             |
| Scan speed/° min <sup>-1</sup>        | 4.0  | 8.0  |
| Measured reflections                  | 2546   | 2574   |
| Unique reflections                    | 2391   | 2433   |
| R <sub>int</sub>                      | 0.022  | 0.032  |
| Obs. reflections with I > 1.0σ(I)     | 1392   | 1704   |
| Parameters                            | 184  | 184  |
| R                                     | 0.052  | 0.039  |
| R'                                    | 0.046  | 0.041  |
| Slope of probability plot             | 1.30   | 1.36   |
| Maximum Δ/σ                           | 0.01   | 0.02   |
| Maximum, minimum Δρ/e Å <sup>-3</sup> | 0.22, -0.28                                    | 0.18, -0.21                                    |

\* Details in common: *M* 256.44, crystal system, monoclinic; λ(Mo-Kα) 0.710 69 Å; *Z* = 4; *F*(000) 544; scan mode ω-2θ; θ<sub>max</sub> 25°.

details are summarised in Table 4. The unit-cell parameters were determined by least-squares refinement from 25 carefully centred high-angle reflections measured at ambient temperature on a Rigaku AFC5S diffractometer. The data were corrected for Lorentz and polarisation effects, but not for absorption. The intensity variations of three check reflections were negligible during the data collections.

Both structures were solved by direct methods by using MITRIL<sup>12</sup> and DIRDIF<sup>13</sup> programs and subsequent Fourier syntheses. Least-squares refinements minimised the function  $\sum w(|F_o| - |F_c|)^2$ , where  $w = 1/\sigma^2(F_o)$ . The neutral atom scattering and dispersion factors were taken from ref. 14. After refinements of all non-hydrogen atoms with anisotropic thermal parameters, the hydrogen atoms were found from a subsequent Fourier difference map for both compounds. Refinements of all atoms, with anisotropic thermal parameters for the non-hydrogen atoms and isotropic ones for the hydrogen atoms, reduced the *R* values to 0.052 (*R'* = 0.046) and 0.039 (*R'* = 0.041) for **1** and **3**, respectively. The greatest maxima in the final Fourier difference map were 0.22 and 0.18 e Å<sup>-3</sup> for **1** and **3**, respectively. All calculations were performed using the TEXSAN<sup>15a</sup> crystallographic software package and the structures plotted with ORTEP.<sup>15b</sup>

Selected bond lengths and angles for the two compounds are shown in Tables 5 and 6, crystallographic data in Table 4, and positional parameters for the *ortho* compound **1** in Table 7 and for the *para* compound **3** in Table 8.

Additional material available from the Cambridge Crystallographic Data Centre comprises H-atom coordinates, thermal parameters and remaining bond lengths and angles.

**Molecular Dynamics Simulations.**—These were performed as previously,<sup>1</sup> except that the version 21.3 of CHARMM was used.<sup>16</sup> The protocol was similar, with equilibration at 450 K.

## Results and Discussion

**Crystal Structures of Compounds 1 and 3.**—The structures of ligands **1** and **3** are shown in Figs. 1 and 2 respectively. The structure of **2** is already available. It is convenient to consider the three structures in terms of SCCSCCS, the so-called 'bracket' unit,<sup>6</sup> which is clearly present (with essentially *anti*-C-C torsions) in the X-ray structure of the free ligands **1**–**3**. It

**Table 5** Selected bond lengths (Å) and angles (°) for compounds **1** and **3**

|                  | <b>1</b> | <b>3</b> |
|------------------|----------|----------|
| S(1)–C(7)        | 1.813(4) | 1.823(3) |
| S(1)–C(8)        | 1.805(5) | 1.823(3) |
| S(2)–C(9)        | 1.818(6) | 1.818(3) |
| S(2)–C(10)       | 1.823(6) | 1.815(3) |
| S(3)–C(11)       | 1.807(7) | 1.825(3) |
| S(3)–C(12)       | 1.805(4) | 1.828(4) |
| C(1)–C(7)        | 1.508(6) | 1.507(4) |
| C(2)–C(12)       | 1.513(5) |          |
| C(4)–C(12)       |          | 1.502(4) |
| C(8)–C(9)        | 1.496(8) | 1.516(4) |
| C(10)–C(11)      | 1.499(7) | 1.514(4) |
| C(7)–S(1)–C(8)   | 99.9(2)  | 101.9(1) |
| C(9)–S(2)–C(10)  | 99.3(3)  | 101.7(2) |
| C(11)–S(3)–C(12) | 100.3(2) | 103.2(2) |
| C(2)–C(1)–C(7)   | 122.9(3) | 120.0(2) |
| C(1)–C(2)–C(12)  | 123.0(3) |          |
| S(1)–C(7)–C(1)   | 115.9(3) | 113.7(2) |
| S(1)–C(8)–C(9)   | 113.9(4) | 113.2(2) |
| S(2)–C(9)–C(8)   | 113.6(4) | 113.5(2) |
| S(2)–C(10)–C(11) | 112.6(4) | 114.0(2) |
| S(3)–C(11)–C(10) | 113.7(4) | 112.3(2) |
| S(3)–C(12)–C(2)  | 116.3(3) |          |
| S(3)–C(12)–C(4)  |          | 113.6(2) |

**Table 6** Selected torsion angles (°) for compounds **1** and **3**

|                        | <b>1</b>  | <b>3</b>  |
|------------------------|-----------|-----------|
| S(1)–C(7)–C(1)–C(2)    | –138.7(3) | 112.0(3)  |
| S(1)–C(8)–C(9)–S(2)    | –158.5(3) | –177.6(2) |
| S(2)–C(10)–C(11)–S(3)  | –167.1(3) | 179.7(2)  |
| S(3)–C(12)–C(2)–C(1)   | 128.4(4)  |           |
| S(3)–C(12)–C(4)–C(3)   |           | –64.2(4)  |
| C(1)–C(7)–S(1)–C(8)    | 58.9(4)   | –47.0(2)  |
| C(2)–C(12)–S(3)–C(11)  | –81.1(4)  |           |
| C(4)–C(12)–S(3)–C(11)  |           | –44.1(3)  |
| C(7)–S(1)–C(8)–C(9)    | 73.5(4)   | 102.6(2)  |
| C(7)–C(1)–C(2)–C(12)   | –4.1(6)   |           |
| C(8)–C(9)–S(2)–C(10)   | 75.8(5)   | 87.2(2)   |
| C(9)–S(2)–C(10)–C(11)  | 73.1(4)   | 86.3(3)   |
| C(10)–C(11)–S(3)–C(12) | 82.0(4)   | 100.2(3)  |

**Table 7** Positional parameters and their estimated standard deviations (e.s.d.s) for compound **1**

| Atom  | x           | y           | z           |
|-------|-------------|-------------|-------------|
| S(1)  | -0.051 5(1) | 0.232 87(8) | 0.003 0(1)  |
| S(2)  | 0.426 8(2)  | 0.324 16(9) | 0.291 0(2)  |
| S(3)  | 0.571 6(1)  | 0.066 4(1)  | 0.221 7(1)  |
| C(1)  | 0.096 1(4)  | 0.079 9(2)  | 0.126 7(4)  |
| C(2)  | 0.243 7(4)  | 0.037 5(2)  | 0.182 2(4)  |
| C(3)  | 0.275 5(5)  | -0.011 8(3) | 0.305 6(5)  |
| C(4)  | 0.164 9(6)  | -0.020 2(3) | 0.371 8(5)  |
| C(5)  | 0.018 2(6)  | 0.019 9(3)  | 0.315 0(5)  |
| C(6)  | -0.014 5(5) | 0.069 3(3)  | 0.195 5(4)  |
| C(7)  | 0.049 4(5)  | 0.134 9(3)  | -0.005 9(5) |
| C(8)  | 0.101 8(7)  | 0.280 5(3)  | 0.158 0(6)  |
| C(9)  | 0.245 8(9)  | 0.312 6(4)  | 0.129 0(6)  |
| C(10) | 0.485 0(6)  | 0.213 8(4)  | 0.323 9(5)  |
| C(11) | 0.554 4(7)  | 0.179 7(4)  | 0.218 3(6)  |
| C(12) | 0.366 7(5)  | 0.037 9(3)  | 0.104 9(5)  |

**Table 8** Positional parameters and their e.s.d.s for compound **3**

| Atom  | x            | y          | z            |
|-------|--------------|------------|--------------|
| S(1)  | -0.334 10(7) | 0.454 7(1) | -0.031 07(4) |
| S(2)  | 0.026 44(7)  | 0.160 7(1) | 0.089 44(5)  |
| S(3)  | 0.150 18(9)  | 0.438 0(1) | 0.328 80(5)  |
| C(1)  | -0.244 0(2)  | 0.659 7(3) | 0.108 4(2)   |
| C(2)  | -0.122 7(3)  | 0.742 0(4) | 0.129 4(2)   |
| C(3)  | -0.043 7(3)  | 0.721 3(4) | 0.206 2(2)   |
| C(4)  | -0.084 6(3)  | 0.613 6(4) | 0.263 9(2)   |
| C(5)  | -0.208 9(3)  | 0.539 1(4) | 0.244 6(2)   |
| C(6)  | -0.288 3(3)  | 0.562 8(4) | 0.168 3(2)   |
| C(7)  | -0.320 4(3)  | 0.667 2(4) | 0.021 3(2)   |
| C(8)  | -0.165 0(3)  | 0.374 2(4) | -0.005 9(2)  |
| C(9)  | -0.143 5(3)  | 0.235 1(4) | 0.060 9(2)   |
| C(10) | 0.095 8(3)   | 0.320 9(4) | 0.167 3(2)   |
| C(11) | 0.078 1(3)   | 0.273 5(4) | 0.252 8(2)   |
| C(12) | 0.007 8(4)   | 0.568 1(6) | 0.342 9(2)   |

was felt that the geometry of the molecules might provide a key to their selectivity. The ligands all appear to have exodentate sulfurs, and yet metal ions are chelated. The five-membered ring chelate is readily formed by a range of metal ions with **1** or **2**. However, ISE studies show that **2** and analogues are more selective for silver.<sup>3</sup> On the hypothesis<sup>3</sup> that this might stem from co-ordination of the two end sulfurs only, an assessment was made of the geometrical requirements for co-ordination to silver. In particular the separations of the non-bonded sulfurs were investigated.

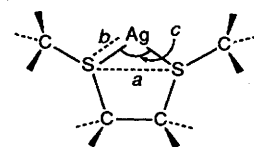
Geometries were extracted from the Cambridge Structural Database (as implemented on CDS at Daresbury) for silver chelates with thioethers. These were averaged to provide consensus geometries. The distances between the non-bonded sulfurs in the crystal structures of the free ligands **1**–**3** are listed in Table 9. These should be compared with the consensus geometries we will now describe. Consider the average separation for two sulfurs in a five-membered chelate ring bonded to silver (a typical motif for crown thioether chelates with metals); the separations obtained from an analysis of 48 structural motifs from the databank or recent literature are averaged in Table 10, to provide a consensus geometry for this motif. The full set of data is given in the Supplementary Data. Also examined were the averaged distances for complexes of **1**–**3** with any metal; there is a greater variance in this set of data, so it was rejected for this study.

Silver has a high tendency to form linear complexes<sup>17</sup> with thiolate or nitrogen ligands. Crystallographically determined distances for two axially co-ordinated thioether sulfurs in the literature are scarce: for a linear S...Ag...S motif a distance of 5.0–5.6 Å would be appropriate. There are linear or almost linear examples of homoleptic silver thiolates, with shorter

**Table 9** Distances between non-bonded sulfurs in crystal structures of compounds **1**–**3**

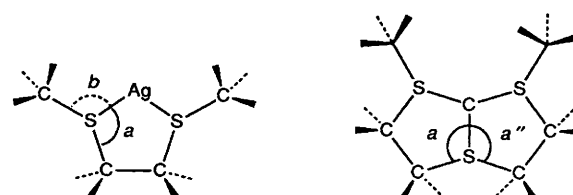
| Ligand   | S(1)···S(2) | S(1)···S(3) | S(2)···S(3) | Ref.      |
|----------|-------------|-------------|-------------|-----------|
| <b>1</b> | 4.398       | 5.772       | 4.421       | This work |
|          | 4.393       | 5.772       | 4.422       | ref. 7    |
| <b>2</b> | 4.494       | 6.841       | 4.422       | ref. 7    |
|          | 4.420*      | 6.608*      | 4.408*      | ref. 7    |
| <b>3</b> | 4.463       | 6.997       | 4.458       | This work |

\* S(4)···S(5), S(4)···S(6) and S(5)···S(6) in ref. 7.

**Table 10** Consensus geometry for silver chelates\*


|                    | $\bar{x}$ | $\sigma_n$ | n  |
|--------------------|-----------|------------|----|
| S–S distance, a/Å  | 2.481     | 0.046      | 48 |
| S–Ag distance, b/Å | 2.700     | 0.150      | 88 |
| S–Ag–S angle, c/°  | 80.86     | 3.39       | 48 |

\* Data extracted from Daresbury CDS files<sup>11</sup> for five-membered chelate rings with thioether donors. See Table S1 of Supplementary Data for full details.

**Table 11** Co-ordination vectors for chelate rings\*


|                 | $\bar{x}$ | $\sigma_n$ | n  |
|-----------------|-----------|------------|----|
| Vector 1        |           |            |    |
| S–Ag distance/Å | 2.595     | 0.051      | 22 |
| Angle a/°       | 98.80     | 2.89       | 22 |
| Angle b/°       | 106.46    | 4.05       | 22 |
| Vector 2        |           |            |    |
| S–Ag distance/Å | 2.667     | 0.074      | 18 |
| Angle a'/a''/°  | 101.04    | 2.99       | 36 |

\* See Table S1 of Supplementary Data for full details.

Ag–S bonds<sup>18</sup> of 2.37–2.42 Å, which should permit S...S distances of 4.74 Å or greater. There is also the 4.7 Å sulfur-to-sulfur distance found by Müller *et al.*<sup>19</sup> for a ten-membered silver–sulfur ring with thiolate bonds to two co-ordinated silver,\* with the angle S...Ag...S 166°. We have also defined an average co-ordination vector from sulfur to silver (from the subset of chelate rings with no bridging sulfurs), to show the direction of bonding potential of the thioether. It is probable that the S...Ag...S angle would be reduced from 180° to permit interaction of the sulfur with silver along this co-ordination vector. Details are shown (Table 11) of the average position found for the five-membered chelate rings accessed. Examples of quasi-axial co-ordination and the six examples of thioether bridging two silvers did not show any obvious trends, and were eliminated from the calculation. These data (shown in

\* The term pseudo-axial will be used in this paper, since the S...Ag...S motif is not usually perfectly linear.

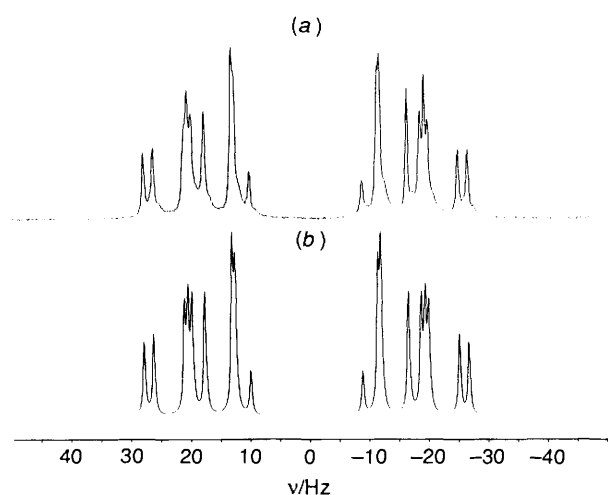
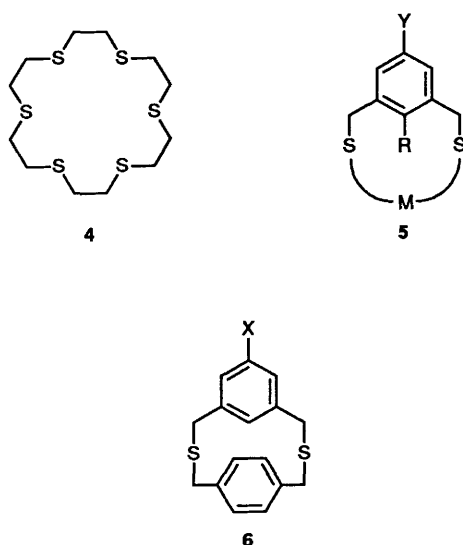


Fig. 3 The AA'BB'  $^1\text{H}$  NMR spectrum of the  $\text{SCH}_2\text{CH}_2\text{SCH}_2\text{CH}_2\text{S}$  section of compound 1: (a) observed and (b) simulated with PANIC



Tables 10 and 11, as extracted from published crystal data in the Cambridge Database<sup>\*,11</sup> or literature as required, using the program QUANTA<sup>20</sup>) have enabled us to set up a consensus geometry for silver. Applying these simple geometric criteria, drawn from experimental data, shows that none of the crystal conformations of the free ligands is a particularly appropriate fit for silver in pseudo-axial co-ordination, nor in a chelate ring.

As pointed out by Bürgi and co-workers<sup>21</sup> many years ago, a crystal structure represents a low-energy conformation, likely to be just one 'snapshot' of a range lying on some reaction coordinate representing conformational or structural change, which might be accessible in fluid phases, and above absolute zero. Indeed, the variability of compound 2 (two different molecules, each disordered in the unit cell), even in the crystal,<sup>7</sup> is an indication of its flexibility. Molecular dynamics simulations permit another method of accessing the rest of the structures on a reaction coordinate for conformational change, and should be especially valuable if started from a crystal structure, which represents a real structure. In solution, the conformations of the free ligands may alter in such a way as to alter the  $\text{S}\cdots\text{S}$  distances found in the crystal structure. The time-scale expected for torsional changes is shorter than the

expected diffusion-controlled encounter rate of ligand and cation in solution complex formation, and is thus pertinent to a discussion of the selectivity of the free ligands. All conformations accessible within picoseconds in solution should be available for interaction with the metal ion in the first step of the co-ordination process. We have attempted to assess the range of conformations accessed with experimental NMR data relating to solution intramolecular processes averaging sections of the ligand, and also to assess the most rapid types of torsional movement of the ligand with MD simulations.

*Conformations in Solution viewed by NMR Spectroscopy.*—Our earlier paper<sup>1</sup> discussed the spectra of the simpler thiocrowns, finding two main ranges of coupling constants, indicative of fluxional molecules with SCCS segments shuttling between *gauche* and *anti* conformations. The equations derived empirically by Abraham and Gatti,<sup>10</sup> relating coupling constants for  $\text{XCH}_2\text{CH}_2\text{Y}$  protons to electronegativities of the substituents X and Y, give rise to the values of  $J_t^g$ , etc. shown in Table 2, and the average coupling constants for particular mixtures are shown in Table 3. These should be compared with the experimental values found in this work (Table 1). In Fig. 3 are shown the experimental spectrum and the spectrum fitted with PANIC for the *ortho* isomer 1 in  $\text{CDCl}_3$ . The results indicate that the ligand is fluxional, with only one apparent AA'BB' spectrum: the coupling constants which were extracted are considerably divergent from those estimated (Table 2) for either *gauche* or *anti* segments, and permit an interpretation similar to that for the hexathiacyclooctadecane 4 studied previously,<sup>1</sup> an average, indicative of a mixture of *gauche* and *anti* segments, here preponderantly *anti*. However, the values for the *meta* and *para* isomers 2 and 3, respectively, are more consistent with an *anti* structure. In each case the spectra indicate just *one* SCCS segment, and thus represent a fluxional molecule. The size of the average coupling constants does indicate that the major components of the molecular ensemble for each of these latter two molecules have an *anti* conformation. The mode of switching must preserve overall the *anti* relation of any two individual protons, and thus does *not* involve simple rotation around the  $\text{S}-\text{C}-\text{S}$  torsion. Studies of the *m*-cyclophane 5 in the 1970s using  $^1\text{H}$  NMR spectra to probe the steric requirements of substituent X, as revealed in the topomerisation process,<sup>22</sup> envisaged the movement of the aryl ring through the macrocyclic ring. For dithiacyclophanes with *two* aromatic rings,<sup>23</sup> for example 6 (M = chain, Y and R are NMR labels), the additional rigidity and ring-current information allowed speculation that a pendulum movement of one aryl ring relative to the second was consistent with the NMR results. Since so much interest was evident from this early work it seemed reasonable to gather conformational information also from the MD method, which used crystal data coordinates as input.

*Molecular Dynamics Simulations.*—Sun and Kollman<sup>24</sup> have recently proposed time-scales for MD simulation of the crown ether 18-crown-6 (1,4,7,10,13,16-hexaoxacyclooctadecane), in order to visualise all major conformations: a series of short 200 ps simulations, each successive one starting from the conformer of lowest energy in the previous simulation; alternatively three successive 2 ns simulations. Both routes produced the major components of the thermodynamic ensemble. Although this was not our main aim in the MD work described here, further work will continue the simulations of our earlier paper<sup>1</sup> and the present one, to provide a more complete set of conformations for the relevant thermodynamic ensembles.

The dynamics data were considered as previously in terms of the time evolution of the torsional angles of the ring, determined for a proportion of saved structures. Another visualisation which for this application is more suitable is to plot the non-bonded sulfur distances for the saved structures. The requisite three distances per simulation are shown in Figs. 4 (all three

\* SERC update January 1992, derived from the Cambridge Database System.

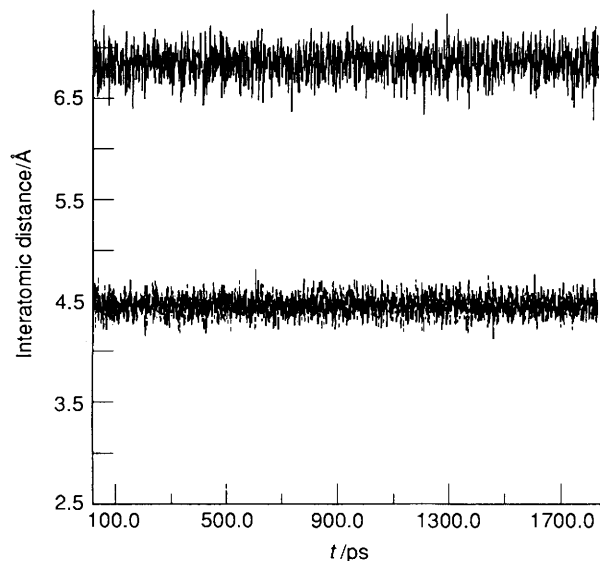


Fig. 4 Time evolution of the three non-bonded distances  $S(1) \cdots S(2)$ ,  $S(1) \cdots S(3)$  and  $S(2) \cdots S(3)$  during MD simulations of ligand 3

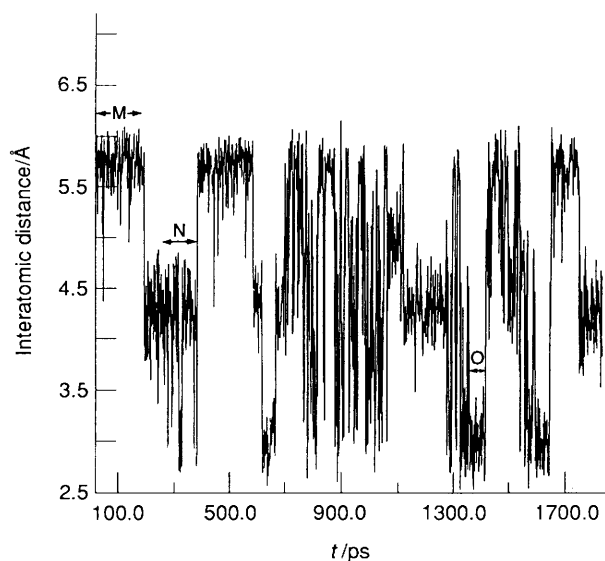


Fig. 5 Time evolution of the non-bonded distance  $S(1) \cdots S(3)$  during MD simulations of ligand 1

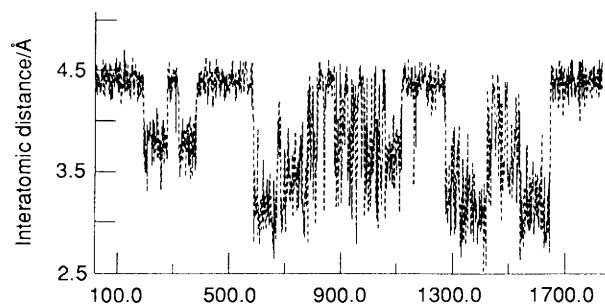


Fig. 6 Time evolution of the non-bonded distance  $S(1) \cdots S(2)$  during MD simulations of ligand 1

distances are shown on one plot for compound 3, 5–7 (separate plots for each distance, for ligand 1) and 8 (superposed plots for ligand 2). These effectively describe the co-ordination profile of each ligand, as it evolves throughout the simulation.

In presenting the data, we have regarded the aromatic ring as static, and viewed the movement of the macrocyclic ring relative to this. To each xylyl segment is fused the SCCSCCS segment

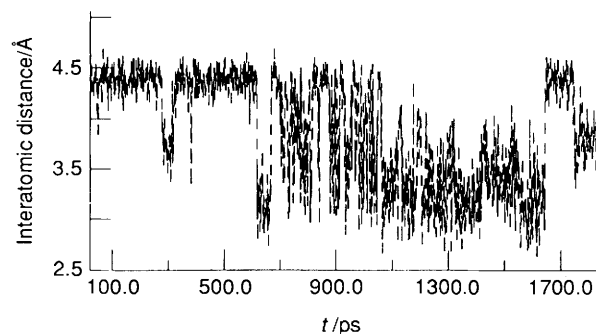


Fig. 7 Time evolution of the non-bonded distance  $S(2) \cdots S(3)$  during MD simulations of ligand 1

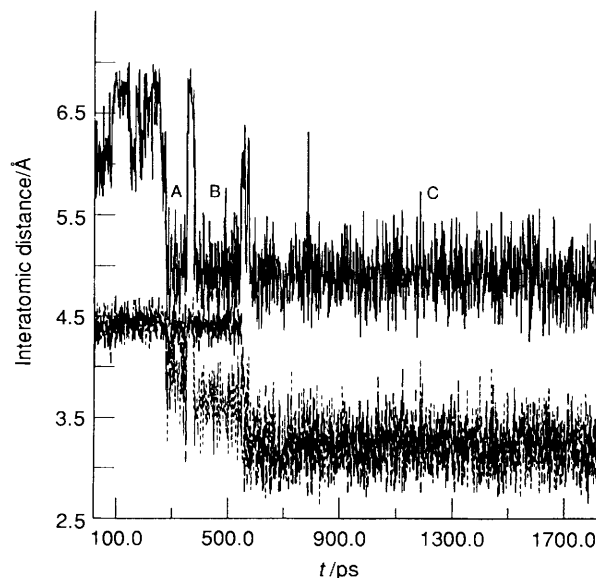


Fig. 8 Time evolution of the three non-bonded distances  $S(4) \cdots S(5)$ ,  $S(5) \cdots S(6)$  and  $S(4) \cdots S(6)$  during MD simulations of ligand 2

which may be viewed as a rope, the sulfurs at the extremities being held at 5.772, 6.608(6.841) or 6.997 Å apart in the crystal structures of 1, 2 and 3 respectively. The NMR data suggest nonetheless that each is mobile, with both sides of the bracket essentially equivalent in solution. The MD work attempts to simulate the movement of the molecule (gas phase, simulated temperature *ca.* 450 K) on a time-scale of a few hundred picoseconds, which should cover processes very much faster than those for which the kinetics can be analysed using rapid NMR techniques. Insight should be gained into the processes which might provide the 'fast' switching seen on the NMR time-scale; also as to the range of conformations the metal ion is likely to interact with in the encounter process of co-ordination, which will be 'slow' by comparison with the ligand torsional changes.

The simulation of the *para* compound 3 is perhaps the most interesting since it indicates very little movement (see Fig. 4) over 1.8 ns in the usual temperature regime we have used. This in fact is the most rigid crown (using this MD criterion) we have yet met. It is more formally 'preorganised' than any other crown examined in our series, which should make it valuable for some as yet undetermined application. Its co-ordination profile is not suitable for intramolecular co-ordination of silver.

The simulation for the *ortho* compound 1 indicates that there is a considerable correlation of the torsional movement of certain portions of the ring, but there appear to be discontinuities. Fuller detail of the correlated movement is given in the Supplementary Data. Viewing the aromatic ring as a pivot, with the ten torsions of the rope numbered as in Fig. 9, the

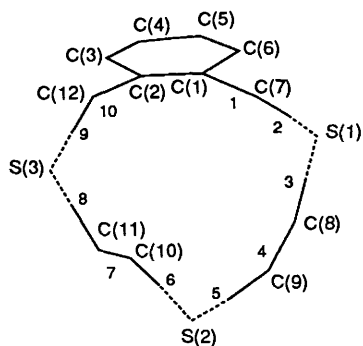


Fig. 9 Labelling of torsion angles in ligand 1

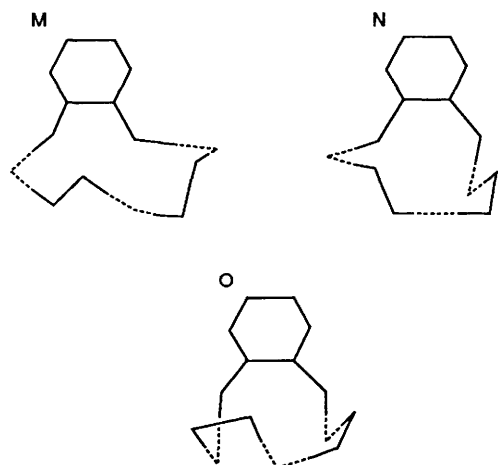


Fig. 10 The 'average' structures of ligand 1 from sections M-O of the trace of S(1)...S(3) in Fig. 5, after energy minimisation with CHARMM

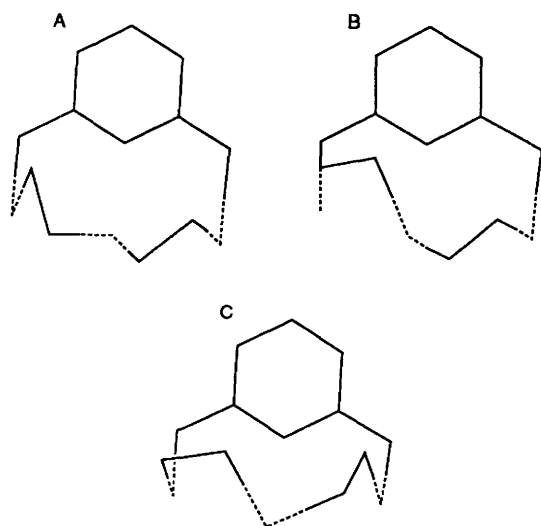


Fig. 11 The 'average' structures of ligand 2 from sections A-C of the trace of S(4)...S(6) in Fig. 8, after energy minimisation with CHARMM, showing two or three sulfurs pointing down from the macrocycle

simulation indicates movements as follows. There are major changes in torsions at *ca.* 200, 260 and 310 ps for all torsions, but some also change significantly at 400, while others change at 430 ps. Torsions labelled 1-4 (as shown on Fig. 9) appear to have synchronised movements; a break in behaviour is observed at torsion 5 which varies only slightly from *gauche* orientations. The 6th and 8th torsions are much more mobile and from the shape of the torsion plots these two appear to have correlated movement. However, in 1800 ps, the two halves of the rope do

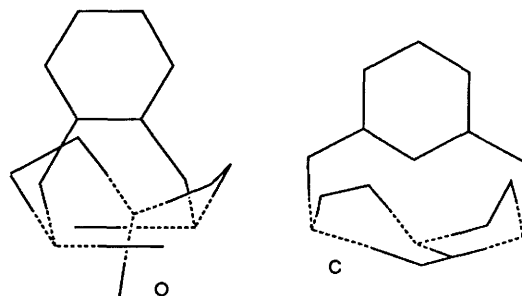


Fig. 12 Representation of the co-ordination vectors for sulfur in structures C and O

Table 12 Energies calculated for the crystal and simulated structures of thiocrowns 1 and 2 (cal = 4.184 J)

| Ligand | Energy/kcal mol <sup>-1</sup> |             | S-C-C-S<br>torsions/ <sup>o</sup> |
|--------|-------------------------------|-------------|-----------------------------------|
|        | MM (CHARMm)                   | MM (ref. 7) |                                   |
| 2      | A                             | 13.8957     | 100.76, -167.0                    |
|        | B                             | 12.8807     | -70.99, -165.78                   |
|        | C                             | 10.5876     | 17.7, -55.47, -57.07              |
|        | Crystal                       | 10.6479     | 11.8                              |
| 1      | M                             | 11.8253     | -176.23, -151.48                  |
|        | N                             | 13.4496     | 172.00, -94.38                    |
|        | O                             | 14.5441     | 19.8, -57.38, -37.60              |
|        | Crystal                       | 11.8253     | 16.8                              |

not become equivalent, as is required by the NMR results, and so a slower process which permits this is still to be observed in a longer simulation. Since the separations between the non-bonded sulfurs of the ligands were regarded as key to their 'organisation' for binding to silver, the MD data are presented to show the time evolution of these separations (see Figs. 5-7), which provides the co-ordination profile of 1. This structure (ligand 1) is very mobile, with sections of the bracket moving independently, to achieve the separation [S(1)...S(2), S(2)...S(3)] of *ca.* 3.5 Å required for co-ordination to silver (Table 10) in a five-membered chelate ring, well within the ps time-scale shown. A proportion of time is spent in other configurations, for example those labelled M, N and O on the plot in Fig. 5. A few picoseconds are spent in the conformation O, with 3.2 Å separations, more suitable for co-ordination to smaller thiophiles, like Pd. No configuration accessed over a significant time-scale had geometrical potential for pseudo-axial co-ordination of silver. It is important to note that the distances plotted do not provide the only criterion which must be met. The averaged structure for a particular metastable section of these plots must be minimised, and the direction of the sulfur co-ordination vectors noted, since these may well prove unsuitable for *chelation* of the desired metal. This is brought out in the representations of the structures in Fig. 10 which shows the minimised average structures for M, N and O on the trace in Fig. 5. Only structure O looks relevant for co-ordination to silver. It is clear that, for this ligand, conformations capable of co-ordinating directly without geometric reorganisation are fleeting. However, ligand reorganisation is likely to occur *after* attack of a metal ion (perhaps at one sulfur), a process we intend to simulate at some later date. Indeed, we have demonstrated positively in earlier work that ligand reorganisation (with breaking of one macrocycle metal link) continues even in a metal-macrocyclic complex.<sup>2</sup> Molecular mechanics energies calculated for all the minimised structures of ligand 1 shown in Fig. 10 are given in Table 12. The lowest-energy conformation M is likely to be the major component of the thermodynamic ensemble for the molecule. It is evident that the torsion angles accessed for the SCCS segments are a *gauche-anti* average, as deduced from the NMR studies.

Finally, for the *meta* isomer **2**, the two S–C–S torsions (4 and 7) are apparently static and *anti* for the first half of the simulation, but around 400 or 550 ps *gauche* metastable structures are observed for each. This molecule shows several pronounced correlated changes of the torsions 1–3 before 270 ps, with two further changes close to 500 ps. The movement is again most easily visualised in terms of the variability of the intramolecular sulfur–sulfur non-bonded distances, the time evolution of which is presented in Fig. 8. In this structure, uniquely for the three free ligands, the co-ordination profile for a considerable part of the simulation (sections A and B in Fig. 8) indicates that two of these sulfurs [S(4) and S(6)]\* are pointing down out of the ring, while the third is pointing up. The latter part of the simulation (C) has all three sulfurs pointing down. Fig. 11 shows the minimised versions of the averaged sections A–C from the traces in Fig. 8, viewed to present this feature, and the MM energies are in Table 12. Since the distance between the sulfurs S(4)···S(6) in sections A–C of Fig. 8 hovers close to  $5.1 \pm 0.3$  Å (the range suitable for S···Ag···S pseudo-axial co-ordination) further graphical study of the underlying structures was made. The direction of an average co-ordination vector for each sulfur as determined from data in Table 11 was applied to the sulfurs of the minimised structures A–C; these offer the possibility of a bent S···Ag···S angle *ca.* 140° or less, which would enable the overlap of silver  $\sigma$ -type orbitals<sup>16</sup> with lone-pair type orbitals on sulfur, and also back donation from Ag to S. If this is the co-ordination mode it may offer a reasonable explanation for the special selectivity of this type of ligand for silver. Few other metals form such long bonds to sulfur, thus the averaged minimised structures for A and B may be incapable of intramolecularly bonding to other metal ions with S(4) and S(6) simultaneously. Structure C, which had the greatest permanence in the study, shows a spectacularly good conformation for co-ordinating facially to silver. On the time-scale occupied by structures A and B on the S(4)···S(6) trace (Fig. 8), one of the other S···S distances approximates to 3.6 Å. Although *apparently* suitable for chelating silver in a five-membered ring, the structures visualised from this section had co-ordination vectors for the third sulfur which were unsuitable for co-ordinating to the same silver ion as the other two. However, fitting the co-ordination vectors from Table 11 to the minimised structure C gives the picture in Fig. 12, inherently capable of co-ordinating silver in a facial manner. Interestingly, the MM energies of the crystal structure (minimised) and C are very similar indeed, see Table 12. Other geometric details for the structures A–C is in Table 12 and Figs. 10–12. The structures observed are not in aggregate consistent with the findings from the NMR analysis of the S–C–S torsions. This can be a result of the thermodynamic ensemble not being fully sampled, which would mean the simulation not matching the experimental, or it could be the experimental effect of solvation on the tendency of the sulfurs to aggregate, which would not be modelled in the simulation process chosen. Future simulations including solvent will address this point. Simulations involving a metal ion ligated by one or more sulfurs would also be of interest.

What does it mean in terms of selectivity? As mentioned earlier, the *meta* ligand **2** presents a remarkable selectivity towards Ag<sup>+</sup> when implemented as a sensor in a poly(vinyl chloride) membrane.<sup>3</sup> The  $K_{Ag,M}^{pot}$  are very low, close to 10<sup>-6</sup> with every metal tested so far, except Hg<sup>2+</sup>, for which the value is close to 10<sup>-3</sup>. We have been unable to obtain good crystals for X-ray diffraction analysis, and consequently we do not know the co-ordination mode of this thio compound with silver in the crystal. However, all sensor experiments with the similar ligands 5-oxa-2,8-dithia[9]-*m*-benzenophane or 2,8-dithia[9]-*m*-benzenophane have shown almost indistinguishable sensor behaviour. This implies that the relevant sulfur atoms involved

in the recognition are S(1) and S(3), that is the sulfurs at the extremities of the rope. Thus it appears (at least with the metacyclophanes) as if the quasi-axial motif is an important factor. Future simulation studies will develop these ideas further, adding silver to the simulations, and investigating the effect of solvation. Work on the electrode implementation of these and related compounds continues.

### Conclusion

Experimental information on three cyclophane ligands in the solid and solution states has been examined to probe the suitability of each to chelate metal ions. A comparison of the geometries of silver chelates, and of metal chelates of these cyclophanes (taken from the CSD), has allowed an hypothesis as to the likely geometry of (a) a five-membered chelate ring and (b) pseudo-axial co-ordination of two sulfurs to silver and (c) the direction of the sulfur co-ordination vector. From MD simulations of compounds 1–3 a series of structures appropriate for chelation types (a) and (b) has been identified for **2** which may be the key to its special selectivity for silver. The co-ordination profile of each ligand has been proposed (Figs. 4–8) and may be efficacious in predicting further selective co-ordinations for other applications. The study of 'preorganisation' of ligand geometry for co-ordination is given a new perspective by the use of MD.

### Acknowledgements

We thank the Spanish Government for funding *via* Comission Asesora de Investigacion Cientifica y Tecnica (CICYT project: MAT88-0179 and MAT91-0952), the Emil Aaltonen Foundation and Suomen Kulttuurirahasto for financial support, and SERC for support. We also acknowledge the use of the SERC funded Chemical Databank Service at Daresbury (January 1992 update) for part of the work described.

### References

- J. C. Lockhart and N. P. Tomkinson, *J. Chem. Soc., Perkin Trans. 2*, 1992, 533.
- J. C. Lockhart, M. B. McDonnell, M. N. S. Hill and M. Todd, *J. Chem. Soc., Perkin Trans. 2*, 1989, 1915.
- J. Casabo, C. Perez-Jimenez, L. Escriche, S. Alegret, E. Martinez-Fabregas and F. Teixidor, *Chem. Lett.*, 1990, 1107; J. Casabo, L. Mestres, L. Escriche, F. Teixidor and C. Perez-Jimenez, *J. Chem. Soc., Dalton Trans.*, 1991, 1969.
- S. R. Cooper and S. C. Rawle, *Struct. Bonding (Berlin)*, 1990, **72**, 1.
- A. J. Blake and M. Schröder, *Adv. Inorg. Chem.*, 1990, **35**, 1.
- R. E. Wolf, J. R. Hartman, J. M. E. Storey, Bruce M. Foxman and S. R. Cooper, *J. Am. Chem. Soc.*, 1987, **109**, 4328.
- B. de Groot and S. J. Loeb, *Inorg. Chem.*, 1990, **29**, 4084.
- NUMARIT, J. S. Martin and A. R. Quirt, *J. Magn. Reson.*, 1971, **5**, 318; version provided by the SERC NMR Program Library, 1981.
- N. Sheppard and J. J. Turner, *Proc. R. Soc. London, Ser. A*, 1959, **252**, 506; R. J. Abraham, *Analysis of High Resolution NMR Spectra*, Elsevier, Amsterdam, 1971.
- R. J. Abraham and G. Gatti, *J. Chem. Soc. B*, 1969, 961; R. J. Abraham, C. J. Medforth and P. E. Smith, *J. Comput.-Aided Mol. Design*, 1991, **5**, 205.
- F. H. Allen, O. Kennard and R. Taylor, *Acc. Chem. Res.*, 1983, **16**, 146.
- C. J. Gilmore, *J. Appl. Crystallogr.*, 1984, **17**, 42.
- P. T. Beurskens, DIRDIF, Direct methods for difference structures, an automatic procedure for phase extension and refinement of difference structure factors, Technical Report 1984/1, Crystallography laboratory, Toernooiveld, Nijmegen, 1984.
- International Tables for X-Ray Crystallography*, Kynoch Press, Birmingham, 1974, vol. 4, Tables 2.2A and 2.3.1.
- (a) TEXSAN-TEXRAY Structure Analysis Package, Molecular Structure Corporation, The Woodlands, TX, 1989; (b) C. K. Johnson, ORTEP, Report ONRL-5138, Oak Ridge National Laboratory, Oak Ridge, TN, 1976.
- B. R. Brooks, R. E. Brucoleri, B. D. Olafson, D. J. States, S. Swaminathan and M. Karplus, *J. Comput. Chem.*, 1983, **4**, 187.

\* We retain the numbering system used in presenting the crystal structure data.<sup>7</sup>



- 17 G. M. Bancroft, T. Chan, R. J. Puddephatt and J. S. Tse, *Inorg. Chem.*, 1982, **21**, 2946.
- 18 K. Tang, M. Aslam, E. Block, T. Nicholson and J. Zubieta, *Inorg. Chem.*, 1987, **26**, 1488.
- 19 A. Müller, M. Römer, H. Bögge, E. Krickemeyer and M. Zimmerman, *Z. Anorg. Allg. Chem.*, 1986, **534**, 69.
- 20 QUANTA 3.0, Polygen Corporation, 1986, 1990.
- 21 P. Murray-Rust, H. B. Bürgi and J. D. Dunitz, *J. Am. Chem. Soc.*, 1975, **97**, 921.
- 22 H. Förster and F. Vögtle, *Angew. Chem.*, 1977, **16**, 429; *J. Chem. Res.*, 1977, (S) 30.
- 23 Y.-H. Lai, *J. Chem. Soc., Perkin Trans. 2*, 1989, 643.
- 24 Y. Sun and P. A. Kollman, *J. Comput. Chem.*, 1992, **13**, 33.

Received 27th March 1992; Paper 2/01627C